

Temperature and energy partition in fragmentation

A. Strachan and C. O. Dorso

Departamento de Física, Facultad de Ciencias Exactas y Naturales,

Universidad de Buenos Aires, Pabellón 1, Ciudad Universitaria, Nuñez

1428, Buenos Aires, Argentina.

Abstract

We study fragmentation of small atomistic clusters via molecular dynamics. We calculate the time scales related to fragment formation and emission. We also show that some degree of thermalization is achieved during the expansion process, which allows the determination of a local temperature. In this way we can calculate the break-up temperature as a function of excitation energy, i.e. the fragmentation caloric curve. Fragmentation appears as a rather constant temperature region of the caloric curve. Furthermore, we show that different definitions of temperature, related to different degrees of freedom, yield very similar values.

I. INTRODUCTION

The highly non equilibrium process of fragmentation, i.e. the expansion and break-up of an excited system, remains of great importance both from the theoretical and experimental points of view. In the field of nuclear physics heavy ion collisions at intermediate energy provide one of the most important examples of this phenomena [1], but the process of fragmentation is also important in other branches of physics, for instance: fragment formation in ion beam or laser ablation sputtering experiments [2], fragmentation of fluids flowing through nozzles, etc. In spite of the great efforts done in order to characterize the process of fragmentation and to understand the mechanisms and instabilities that lead to the break-up, several aspects remain obscure. Most noticeable, the possible relation of this process with the liquid-gas phase transition or critical phenomena are, at present, not clearly understood.

One of the main present lines of research is focused on the determination of the temperature of the fragmenting system at break-up time which, when analyzed in terms of the excitation energy leads to the the nuclear fragmentation caloric curve. The meaning of temperature and the interpretation of the caloric curve in fragmentation processes face two important problems. On the one hand the systems are usually very small (~ 100 constituents). This is not a serious problem, at least for low excitation energies when the small system is self-confined; it has been recently shown that very small systems can undergo phase transitions [22] and calorimetric experiments have been done in systems as small as 139-particle Na clusters [21]. The second problem is related to time, the expanding system and the clusters are transient systems. This is the same problem that appears when studying isolated liquid clusters; fortunately the metastable states usually live long enough to be measured. This said, let us mention some of the recent efforts to calculate the fragmentation caloric curve, i.e. temperature as a function of energy. Pochodzalla et al. [3] have calculated the “isotope temperature” as a function of the total energy per nucleon in different nuclear reactions. They calculated the “isotope temperature” in experiments performed by the ALADIN collaboration. Isotope temperature is computed from ratios of clusters yields, assuming that

the system is at low density and that thermal and chemical equilibrium is achieved [4]. In the fragmentation region they find two behaviors: in the energy range 3 MeV to 10 MeV the temperature remains almost constant with a value of ~ 5 MeV. The temperature value of this plateau coincides with the limiting excitation energy per nucleon for fusion-evaporation process. For excitation energies beyond 10 MeV they find a steady increase of the isotope temperature. Comparing this caloric curve with the one characteristic of liquid-gas phase transition in the thermodynamic limit, the behavior for high energies, was related to the presence of the nuclear “gas phase”, the region of increasing temperature, for high energies in the fragmentation caloric curve will be called “gas branch”. In numerical simulations, using a quantum molecular dynamics model for the study of fragmentation [5], a similar behavior is found for the temperature of the gas of fragments, although some criticisms can be raised against the later calculations regarding the way the collective expansion is taken into account. Recently the isotope temperature was calculated by the EOS collaboration for Au on C central collisions. The plateau is confirmed but the rise at high energies, i.e. the “gas branch”, is not found [6]. In very recent experiments [7] the “emission or excited-state temperature” was calculated over a wide excitation energy on Au+Au reactions. Contrary to the results is [3], the emission temperature is rather constant throughout the whole energy range, and does not increase for high energies. For an excellent review on the calculation of the caloric curve in nuclear reactions and the different definitions of temperature see [1]. In simulations of fragmentation of two dimensional classical systems via molecular dynamics, the fragmentation regime appears, also, as a flat region in the caloric curve [8]. It is thus very important to understand the fragmentation caloric curve, in particular to understand its high energy behavior, and check whether the “gas phase” behavior, i.e. the gas branch, is seen or not.

In this paper we study the fragmentation of excited classical Lennard-Jones (L-J) drops, formed by $N = 147$ particles, simulated via molecular dynamics. We chose L-J pair potential because it is a general potential featuring short-range repulsion and longer-range attraction, which is needed for clusterization to happen. The equation of state of L-J systems displays

Van der Waals behavior as is expected for nuclear systems. Fragmentation in L-J drops has been studied extensively by many authors [9–12], this simple model has given a lot of information about the process of fragmentation. Understanding the process of fragmentation in classical LJ drops does not mean understanding nuclear multifragmentation, but it is unlikely that we will understand the nuclear process if we do not understand it in the simple LJ case.

The main purpose of this work is to show that we can define a “local temperature” of the fragmenting system which achieves some degree of local equilibrium after a very short period of time. Also, we developed a way to define precisely the time at which the fragments are formed. Thus we can calculate the break-up temperature in fragmentation, from which we can calculate the caloric curve of our L-J system in a very wide energy range, encompassing the solid-like and liquid-like phases (and the associated phase transition) and, more important to us, evaporation and fragmentation processes.

In order to unveil the mechanisms that lead to the fragmentation of an expanding system, it is mandatory to know the times at which fragments are formed and emitted. We pay particular attention to the calculation of the time-scales related to cluster formation and emission, as we will see this is important to the physical meaning of the “local temperature”.

Another characteristic feature of fragmenting systems is the development of a collective expansion or radial flux. Identifying this collective motion correctly, is essential to calculate temperature. We study the way in which the total energy is partitioned into potential energy (V), collective kinetic energy (K_{coll}), associated to the radial flux, and internal kinetic energy (K_{int}) as a function of time and for different total energies of the system. We will then see how two local temperatures can be defined, one related to the fluctuations of the velocity of the particles over the radial, collective motion, and the second related to the fluctuations of the center of mass velocities of the clusters. The internal temperature of the clusters is also calculated as a function of the fragment mass, for different times. The relation among the different temperatures is analyzed.

This paper is organized as follows: in section II we will describe the model that we use

to simulate the fragmentation process. In section III is devoted to the study of fragment formation and emission time-scales, followed by our results on the properties of the asymptotic fragments in section IV. Section V deals with the energy partition, and in section VI we show the caloric curve for our Lennard-Jones system in a wide energy range encompassing fragmentation and also the solid-like and liquid-like phases. Finally, in section VII, conclusions are drawn.

II. COMPUTER EXPERIMENTS

As stated in the Introduction we study fragmentation of excited Lennard-Jones drops. The two body interaction potential is taken as the truncated Lennard Jones (6-12) potential:

$$V(r) = \begin{cases} 4\epsilon \left[\left(\frac{\sigma}{r}\right)^{12} - \left(\frac{\sigma}{r}\right)^6 - \left(\frac{\sigma}{r_c}\right)^{12} + \left(\frac{\sigma}{r_c}\right)^6 \right] & r < r_c \\ 0 & r \geq r_c \end{cases} \quad (1)$$

We took the cut-off radius as $r_c = 3\sigma$. Energy and distance are measured in units of the potential well (ϵ) and the distance at which the potential changes sign (σ), respectively. The unit of time used is: $t_0 = \sqrt{\sigma^2 m / 48\epsilon}$. We used the well known Verlet algorithm to integrate the classical equations of motion [13] taking $t_{int} = 0.001t_0$ as the integration time step. This led to energy being conserved approximately one part per million.

We performed explosions of $N = 147$ particles, three dimensional drops. The initial configurations are constructed by cutting a spherical drop from a thermalized, periodic, Lennard-Jones system with $N = 512$ particles in each periodic cell. The degree of excitation can be easily controlled in this way by varying the density and temperature of the periodic system. The initial state of our drops is macroscopically characterized by their energy and density (taken as that of the periodic system). We studied a broad energy range which encompasses very different behaviors regarding the fragmentation pattern, going from $E = -2.4\epsilon$ to $E = 2.2\epsilon$. The density was taken as $\rho = 0.85\sigma^{-3}$ for energies in the range $E = -1.5\epsilon$ to $E = 2.2\epsilon$, and for $E = -2\epsilon$ we studied the cases $\rho = 1\sigma^{-3}$ and $\rho = 1.09\sigma^{-3}$. The temperature of the periodic system used for constructing the initial configurations is

in the range ~ 1.4 to $\sim 4.3\epsilon$. From the equation of state of the Lennard-Jones system [14], it can be seen that our initial drops are in a hot and compressed. For each energy we performed and analyzed no less than 120 explosions, for $E = 1.8\epsilon$, $E = 0.9\epsilon$, $E = 0.5\epsilon$ and $E = -0.5\epsilon$ we studied 300 evolutions.

III. FRAGMENT FORMATION AND EMISSION

As stated in the introduction, many systems, differing greatly in size, interaction potential, etc, exhibit fragmentation. Thus, a good way of characterizing the excitation of the system is according to the asymptotic mass spectra. If the energy of the system is high, it will break in several small fragments. The asymptotic mass spectrum will show rapid decay for large masses. On the other hand, for low excitation energies, the system will evaporate monomers and small clusters while a big drop, comprising most of the mass of the system, will remain bound. In this case the mass spectrum is U shaped. A third case is usually found: for a given intermediate energy the mass spectrum will show power law behavior. This last case is quite important. Taking into account that a power law implies scale invariance, and power law mass spectra are found in second order phase transitions, (e.g. percolation at the critical probability [15] or liquid-gas phase transition at the critical point [16]), the power law mass spectra was associated with the system undergoing a second order phase transition [17]. This conjecture, however attractive, has not been confirmed.

In Fig. 1 we show the asymptotic mass spectra for six different energies, namely $E = 2.4\epsilon$, $E = 1.8\epsilon$, $E = 0.9\epsilon$, $E = 0.5\epsilon$, $E = -0.5\epsilon$, and $E = -2.4\epsilon$. The general behavior described in the last paragraph can be seen in Fig. 1. Although we are not interested in checking the occurrence of a second order phase transition, we can see that the power law mass spectra must be close to $E = 0.5\epsilon$.

In order to study the mechanisms that lead to fragmentation it is important to know the time at which the asymptotic fragments form and the one at which they are emitted.

In previous papers we have fully analyzed the main fragment recognition algorithms

currently in use, see for example [18]. The simplest definition of cluster is basically: a group of particles that are close to each other and far away from the rest. The fragment recognition method known as minimum spanning tree (MST) is based on the last idea [18]. In this approach a cluster is defined in the following way: given a set of particles i, j, k, \dots , they belong to a cluster C if :

$$\forall i \in C, \exists j \in C / |\mathbf{r}_i - \mathbf{r}_j| \leq R_{cl} \quad (2)$$

where \mathbf{r}_i and \mathbf{r}_j denote the positions of the particles and R_{cl} is a parameter usually referred to as clusterization radius, and is usually related to the range of the interaction potential. In our calculations we took $R_{cl} = 3\sigma$.

On the other hand, the early cluster formation model (ECFM) [19], is based on the next definition: clusters are those that define the most bound partition of the system, i.e. the partition (defined by the set of clusters $\{C_i\}$) that minimizes the sum of the energies of each fragment:

$$E_{\{C_i\}} = \sum_i \left[\sum_{j \in C_i} K_j^{cm} + \sum_{j, k \in C_i} V_{j, k} \right] \quad (3)$$

where the first sum is over the clusters of the partition, and K_j^{cm} is the kinetic energy of particle j measured in the center of mass frame of the cluster which contains particle j . The algorithm (early cluster recognition algorithm, ECRA) devised to achieve this goal is based on an optimization procedure in the spirit of simulated annealing [19].

It has long been known that the ECRA algorithm finds that the asymptotic clusters are formed, in phase space, long before the separate in coordinate space, and become recognizable with the MST algorithm, i.e. long before they are emitted [20,12,18]. We then associate the time at which the ECRA method finds the asymptotic clusters to the fragment formation time-scale and the one related to the MST analysis to the fragment emission time-scale. We will devote the rest of this section to the calculation of the above mentioned time-scales.

In Fig. 2 we show the time evolution of the mean mass of the greatest fragments, Fig. 2(a), and the intermediate mass fragments (fragments with mass in the range 4 - 50)

multiplicities, Fig. 2 (b), obtained using both fragment recognition algorithms. It is clear that the ECRA recognizes the asymptotic fragments before they separate in coordinate space.

Another important quantity is the microscopic stability of the clusters. In order to study this we define the following microscopic persistence coefficient. At a given time t the system will be formed by a set of clusters $C_i(t)$ which will become, for long times, the asymptotic fragments which we will denote C_i . Lets consider a given cluster $C_i(t)$ with mass number $n_i(t)$, let $b_i(t) = n_i(t)(n_i(t) - 1)/2$ be the number of pairs of particles in the cluster. Its constituents particles might be at the asymptotic time in two or more different clusters. We define $a_i(t)$ as the number of pairs of particles that belong to $C_i(t)$ and also are together in a given asymptotic cluster. We are now able to define the microscopic persistence coefficient

$$P(t) = \frac{1}{N_{ev}} \sum_{ev} \left[\frac{1}{\sum_{cl} m_i(t)} \sum_{cl} m_i(t) \frac{a_i t}{b_i t} \right], \quad (4)$$

where the first sum runs over the different events for a given energy, N_{ev} is the number of events, and the other two sums run over the clusters at time t . It is clear that the persistence coefficient is equal to 1 if the microscopic structure of the clusters is equal the the asymptotic one. On the other hand this coefficient approaches 0 when the two partitions under study bear little similarity. This coefficient can be defined for ECRA clusters as well as for MST ones. In Fig. 3 we show $P(t)$ for the ECRA analysis (full lines) and $P(t)$ for the MST analysis (dashed lines). In each case the asymptotic partition was taken as that resulting from the corresponding analysis (ECRA or MST) for time $t = 150t_0$. At this “asymptotic” time ECRA and MST analysis yield almost the same results. The horizontal lines in Fig. 3 represent a reference value related to an evaporation-like process. It is the value of the persistence coefficient when each asymptotic partition is compared with itself after removing one particle from each of it constituents clusters of mass number greater than 2, i.e.:

$$P_{ref} = \frac{1}{N_{ev}} \sum_{ev} \left[\frac{1}{\sum_{cl} m_i(t_\infty)} \sum_{cl} m_i(t_\infty) \frac{m_i(t_\infty)(m_i(t_\infty) - 1)}{(m_i(t_\infty) - 1)(m_i(t_\infty) - 2)} \right], \quad (5)$$

where the second sum runs over clusters of mass 3 and above and $m_i(t_\infty)$ denotes the mass number of cluster i which belongs to the asymptotic partition.

We can define, from the results shown in Figs. 2 and 3, two different time scales: a “break-up or fragment formation time” $\tau_{ff}(E)$ related to the ECRA partition differing from the asymptotic partition by an evaporation-like process, and a “fragment emission time” τ_{fe} given by the time at which the asymptotic fragments separate from each other, and consequently the MST partition differs from the asymptotic one by an evaporation-like process. We obtain the following time-scales: $\tau_{ff}(1.8\epsilon) \sim 20t_0$, $\tau_{ff}(0.9\epsilon) \sim 35t_0$, $\tau_{ff}(0.5\epsilon) \sim 52t_0$, $\tau_{ff}(-0.5\epsilon) \sim 75t_0$. It is important to note that at the above times the system is already broken in phase space (ECRA analysis) but not fully broken in coordinate space (MST analysis), and the biggest MST cluster contains more than half the total mass of the system, see Figs. 2 and 3. This last fact will turn out to be important in order to characterize the break-up state of the system.

We obtained the following time-scales for fragment emission: $\tau_{fe}(1.8\epsilon) \sim 40t_0$, $\tau_{fe}(0.9\epsilon) \sim 60t_0$, $\tau_{fe}(0.5\epsilon) \sim 67t_0$, $\tau_{fe}(-0.5\epsilon) \sim 100t_0$.

IV. INTERNAL TEMPERATURE OF THE FRAGMENTS

The internal state of the asymptotic clusters is a very important quantity in fragmentation. The reason is twofold, on the one hand the asymptotic excitation of the clusters is accessible experimentally in nuclear fragmentation [7] and in small atomistic clusters [21]. On the other hand, as we will show, the internal temperature of the asymptotic clusters gives information about the break-up state of the system. We calculate the internal temperature of the clusters of mass number $n > 1$ in the following way:

$$T_{cl}(n) = \frac{1}{N(n)} \sum_j \frac{1}{3n-3} \sum_{i \in j} \frac{1}{2} m(v_i^{j-cm})^2, \quad (6)$$

where $N(n)$ is the number of clusters of mass number n in all events for a given energy, the first sum runs over all clusters j of mass n , the second sum runs over the particles i belonging to cluster j and v_i^{j-cm} denotes the velocity of particle i measured from the c.m. frame of the cluster it belongs to.

In Fig. 4(a) we show the internal temperature of the asymptotic clusters ($T_{cl}(n)$) as a function of its mass number for the wide range of energies considered; in Fig. 4(b) the same quantity is plotted but at fragment formation time ($\tau_{ff}(E)$), in this last case we used the ECRA clusters. Fig. 4 shows a very important result: the temperature of the asymptotic clusters depends only on their mass, and not on the total energy of the fragmenting system, furthermore at break-up time τ_{ff} the temperature of the fragments is basically equal to that of the asymptotic ones. This means that at break-up time the clusters have already cooled down to a long lived metastable state in which they need no further relaxation, except for little evaporation. For times greater than $\tau_{ff}(E)$, the clusters simply fly away from each other but nothing really important happens regarding their internal degrees of freedom, except, again, for some evaporation. The same behavior was found for two dimensional Lennard Jones drops [8]. Let us mention that the energies shown in Fig. 4, represent very different behaviors regarding the fragmentation pattern, it can be seen that for $E = 1.8\epsilon$ there are no clusters of mass bigger than ~ 30 , while for $E = -0.5\epsilon$ there are little intermediate mass fragments, which comes from a U-shaped mass spectra.

V. ENERGY PARTITION: COLLECTIVE EXPANSION, INTERNAL KINETIC AND POTENTIAL ENERGIES

In order to study the development of the collective flux and the way the total energy is partitioned we take the following approach. Since the radial collective velocity is position dependent, the outer particles expand at a faster rate than the inner ones, we divide our drops in concentric spherical regions. The i^{th} region, is formed by the points \mathbf{r} in coordinate space that satisfy:

$$\delta r (i - 1) \leq |\mathbf{r}| < \delta r i \quad (7)$$

where δr is the width of the regions, we took $\delta r = 2\sigma$. \mathbf{r} is measured from the c.m. of the system, as will be any coordinate position throughout the paper.

We now define the mean radial velocity of region i as:

$$v_{rad}^{(i)}(t) = \frac{1}{N_i(t)} \sum_{ev} \sum_{j \in i} \frac{\mathbf{v}_j(t) \cdot \mathbf{r}_j(t)}{|\mathbf{r}_j(t)|} \quad (8)$$

where the first sum runs over the different events for a given energy, the second over the particles j that belong, at time t , to region i and \mathbf{v}_j and \mathbf{r}_j are the velocity and position of particle j . $N_i(t)$ is total number of particles belonging to region i in all the events.

We can divide the total kinetic energy per particle in two parts:

$$K(t) = K_{coll}(t) + K_{int}(t). \quad (9)$$

The term $K_{coll}(t)$ is related to the collective motion:

$$K_{coll}(t) = \frac{1}{n_{ev}N} \sum_{regions} N_i(t) \frac{m}{2} \left(v_{rad}^{(i)}(t) \right)^2 \quad (10)$$

where m is the mass of each particle, n_{ev} is the number of events and $N = 147$ is the number of particles in each drop. The second term, $K_{int}(t)$ is related to the “internal” kinetic energy:

$$K_{int}(t) = \frac{1}{n_{ev}N} \sum_{regions} \sum_{j \in i} \frac{1}{2} m \left(\mathbf{v}_j - v_{rad}^{(i)} \cdot \hat{\mathbf{r}}_j \right)^2 \quad (11)$$

where $\hat{\mathbf{r}}_j = \mathbf{r}_j / |\mathbf{r}_j|$.

In Fig. 5 we show $K(t)$, $K_{coll}(t)$, $K_{int}(t)$ and the potential energy, $V(t)$, as a function of time, for four different cases. During the initial stage of the fragmentation process the collective expansion builds up, while the internal kinetic energy diminishes, i.e. the system relaxes. The potential energy grows in time because the system is fragmenting and consequently increasing its surface.

In order to see the way in which the mean radial velocity depends on position, we show in Fig. 6 the radial velocity profiles $v_{rad}^{(i)}(\tau_{ff})$ at break-up time, for the same energies as in Fig. 5. The position dependence is clear and so is the fact that the expansion velocity increases with the total energy.

What we defined as the internal kinetic energy can be related to “local temperature” which is usually defined as the velocity fluctuations around the mean collective velocity, which in our case is the mean radial velocity [23], i. e.:

$$T_{loc}^{(i)} = \frac{1}{N_i(t)} \frac{2}{3} \sum_{j \in i} \frac{1}{2} m \left(\mathbf{v}_j - v_{rad}^{(i)} \cdot \hat{\mathbf{r}}_j \right)^2, \quad (12)$$

In this way we are making the conjecture that the fragmenting system is in local equilibrium and the velocity distribution follows [23]:

$$f(\mathbf{v}; \mathbf{r}) = \rho(\mathbf{r}) \left(\frac{m\beta(\mathbf{r})}{2\pi} \right)^{3/2} e^{\beta(\mathbf{r}) \frac{m}{2} (\mathbf{v} - \mathbf{v}_{rad}(\mathbf{r}))^2} \quad (13)$$

where $\rho(\mathbf{r})$ and $\beta(\mathbf{r})$ are the local density and inverse of the local temperature respectively; $\mathbf{v}_{rad}(\mathbf{r})$ is the collective velocity which in our case is in the radial direction. In Fig. 7 we show the local temperature profiles for different energies, namely $E = 1.8\epsilon$ (full lines), $E = 0.9\epsilon$ (dotted lines), $E = 0.5\epsilon$ (dashed lines) and $E = -0.5\epsilon$ (dashed-dotted lines), and for different times. In Fig. 7(a) full symbols denote the local temperature profiles at break-up time and empty symbols correspond to the initial configuration, i.e. $t = 0$ and in Fig. 7(b) full symbols denote, again, break-up time and empty symbols correspond to asymptotic times. In order to check validity of the local equilibrium conjecture and the physical meaning of the local temperature we analyzed the degree of isotropy of the velocity fluctuations around the expansion. We found that the local temperature related to velocity fluctuations in the radial direction is equal to that related to transverse fluctuations. As a consequence the expanding system can be considered to be in local equilibrium at τ_{ff} .

From Fig. 7 we can clearly see that while the initial temperature profiles are quite different in the cases shown (corresponding to very different excitation energies) the local temperature profiles at break-up time are quite similar in all the cases. In this way we can characterize the velocity distribution at the break-up state as a mean radial velocity, which grows almost linearly with distance from the c.m. of the system, and which depends on the total energy of the system plus velocity fluctuations, on top of the collective motion, which do not depend on the total excitation of the system. This result is important because it represents the first step in the characterization of the break-up state. At this point the central problem is understanding why the local temperature at break-up is the same for all initial conditions (i.e. excitation) and what is the meaning of its value. We will devote

next section to answer that question. It is also interesting to note the no evidence of “gas phase” phase behavior, i.e. the increase of temperature for high energies, is found for the local temperature.

In Fig. 8 we show the time evolution of the local temperature averaged over the three innermost regions (which comprise approximately the volume of the initial drop) for different energies. It can be seen that during the first stage of the fragmentation process part of the initial thermal energy of the system is converted to collective energy and the local temperature decreases. This process continues until a given temperature is achieved, this value of temperature is quite independent of the total energy of the system, but it can be seen that it slowly diminishes as the total energy increases. It is worth mentioning at this point that the energies shown in Fig. 8 represent very different behaviors of the system regarding its asymptotic states, see the mass spectra in Fig. 1. A similar behavior was found for classical two dimensional drops [8].

We now focus our attention on the way the total energy of the system is partitioned. The partition of energy as a function of the total energy of the system is undoubtedly important for the understanding of the process of fragmentation. in Fig. 9(a) we show the asymptotic values of collective and internal kinetic energy, the potential energy and the average local temperature of the three inner most region as a function of the total energy. Perhaps more important that the asymptotic values are those at the break up time. In Fig. 9(b) we show the same quantities, see caption for details, but for the break-up time $\tau_{ff}(E)$. It can clearly be seen that the local temperature at break-up is quite independent of the total energy, in contrast with the other quantities that vary noticeably in the energy range shown. Furthermore it is very interesting to note that this value of the local temperature is very similar to the internal temperature of the greater clusters, see Fig. 4. The meaning of the constancy of the local temperature and of its value will become apparent in the next section.

As already mentioned in the introduction we can define a cluster local temperature related to the fluctuations of the c.m. velocity of the clusters over the collective expansion:

$$T_{clloc}^{(i)}(t) = \frac{2}{3N_i(t)} \sum_{j \in i} \frac{1}{2} m \left(\mathbf{v}_{cm}^{(j)} - \frac{\mathbf{v}_{rad}^{(i)} \cdot \mathbf{r}_{c.m.}^{(j)}}{|\mathbf{r}_{c.m.}^{(j)}|} \right)^2 \quad (14)$$

where the sum runs over the clusters whose c.m. position belongs to the i^{th} region in all the events, $\mathbf{v}_{cm}^{(j)}$ is the c.m. velocity of cluster j and $\mathbf{r}_{cm}^{(j)}$ is, of course, the position of the c.m. of the cluster. We will use the name “local temperature” for the one related to fluctuations of the particle velocities and “cluster local temperature” for the one defined in the last equation.

In Fig. 10 we show the cluster local temperature profiles for energies $E = 1.8\epsilon$, $E = 0.9\epsilon$, $E = 0.5\epsilon$ and $E = -0.5\epsilon$ at break-up time. The profiles are similar to those of the local temperature, Fig. 7. Taking into account that the number of clusters is much smaller than the number of particles the values plotted are more likely to deviate from their mean value. This quantity is very important because contrary to the local temperature it can be measured in experiments, at least at asymptotic times [1]. Again, no evidence of the “gas branch” is found.

VI. EXTENDED CALORIC CURVE

In this section we show the caloric curve for our 3 dimensional L-J drops, Fig. 11, in a very wide energy range. The “extended caloric curve”, as we will name it, encompasses the solid-like phase (region I), the liquid-like phase (region III), the associated phase transition (region II), and also the higher energy process of evaporation and multifragmentation (region IV).

The low energy part of the caloric curves (regions I, II and III) was obtained by analyzing MD simulations whose initial configurations were obtained by rescaling the velocities of a $N = 147$ particles drop originally constructed close to its ground state. This low energy configuration was obtained simply by cutting a spherical drop from a FCC crystal, whose density was taken as the close-packed one ($\rho \sim 1.091/\sigma^3$) and whose temperature was close to zero. Once this initial configuration was cut the particle velocities were set to zero and

the system was evolved for a long time to achieve thermalization. In order to study the drop for different energies, the velocities of the thermalized low energy system were rescaled so as to get the desired total energy. At the low energies in the range encompassed by regions I, II and III of Fig. 11 the LJ system is self confined except for some little evaporation at the higher energies of region III. The temperature in regions I, II and III is related to c.m. kinetic energy of the drop, disregarding any evaporated particle.

In region IV we plot the local temperature averaged over the three inner most regions from our fragmentation computer experiments, also averaged over a time $t = 20t_0$ centered at the break-up time, see Fig. 7. This means that the extended caloric curve in the fragmentation region represents the break-up temperature of the system. Let us mention that at break-up time the three central regions contain ~ 60 to ~ 90 particles, and a big, interacting, MST cluster is still present, see Fig. 2.

Regions I, II and III feature the well known solid-like to liquid-like phase transition in small systems [22]. In region I the drop is solid, the solid-liquid phase transition appears as the loop in region II. In region III the drop is liquid-like. In this low energy regime the behavior of the drops resemble that of the macroscopic systems, although there are some important differences, see [22]. It is clear that an isolated liquid drop cannot be heated without limits. Once a certain temperature is attained, which depends on the size of the system, if more energy is supplied to the system it will evaporate particles but it will not heat up; we will call this temperature the limit temperature T_{lim} . This feature can be seen in the high energy region of region III. For energies higher than that of the evaporating liquid the system undergoes the non equilibrium process of fragmentation, region IV of Fig. 11. Of course the limit between evaporation and fragmentation (regions III and IV) is arbitrary. Due to this “overlap”, for $E = -2\epsilon$ we performed evolutions applying the velocity rescaling method used for studying low energy drops and also constructing the initial configurations from the periodic system, i.e. the method used to study fragmentation. It is important to notice from Fig. 11, $E = -2\epsilon$ that we obtained the same value of temperature regardless of the way we constructed the drop and the definition of temperature used.

It is worth mentioning again that the caloric curve in the fragmentation region represent the local temperature of the central regions of the expanding system at break-up. This process appears as a quite constant temperature region of the caloric curve, decreasing slowly for high energies. It can be seen from Fig. 11 and from the temperature profiles, Fig. 7, that the local temperature at break-up is quite independent of the total energy of the fragmenting system. Note that the initial drops in our fragmentation computer experiments (described in section II) are artificially constructed hotter than the limit temperature, in real cases this state is achieved via a sudden input of energy like in collisions. In its evolution the system cools down, while the expansion builds up, until it reaches the limit temperature, which of course does not depend on the initial excitation of the system, and needs no further relaxation. From this time on the system continues its expansion at constant velocity and the temperature remains quite constant. The slow decrease of the temperature for high energies is related to the fact that the size of the drops diminishes (as the system breaks into more fragments) and consequently their limit temperature decreases too. Within this picture we can understand why the internal temperature of the fragments, from τ_{ff} on, is independent of the initial excitation of the system, Fig. 4. The system expands until it needs no further relaxation, which means that the fragments will be “as hot as they can”. Notice that the internal temperature of the big clusters is very similar to the limit temperature of the $N = 147$ drop.

VII. DISCUSSION

The fragmentation process can be divided in three stages. The first one which we will call flux and fragment formation stage, goes from $t = 0$ to $t = \tau_{ff}(E)$. During this stage the radial flux and density fluctuations develop, these elements determine the cluster partition according to the ECFM model. By the end of this stage the asymptotic fragments are already formed although most of the mass of the system is still interacting and forming a big configurational (MST) cluster. During this stage and while the collective motion develops

the system cools down. We showed that some degree of local equilibrium is achieved and that a local temperature can be defined. At τ_{ff} the local temperature profiles are quite independent of the total energy of the system, of course the initial profiles depend on the total energy of the system and on the initial density. The value of the local temperature in the central region of the drop is equal to the limit temperature of its constituents clusters, i.e. the maximum internal temperature that the liquid clusters can have. This means that the initial cooling process continues until the temperature attains its limit value and the system needs no further relaxation. This is why the local temperature at break-up is quite independent of the total energy, and it slowly decreases when the total energy increases; as the total energy of the system increases it breaks into smaller clusters and consequently the limit temperature diminishes.

The second stage of the fragmentation process, which we will name fragment emission stage, goes from $\tau_{ff}(E)$ to $\tau_{fe}(E)$. During this stage the already formed fragments are emitted, i.e. they separate in configurational space and become recognizable with a MST cluster analysis. The local temperature profiles are quite constant during this second stage (Fig. 7(b)) and so is the internal temperature of the clusters, Fig. 4. Most of the cooling and relaxation has already taken place during the fragment and flux formation stage.

The third stage encompasses times greater than τ_{fe} and will be called free expansion stage. During this stage the already emitted clusters expand freely. Only some evaporation may occur.

We have also studied the cluster local temperature, related to the clusters c.m. velocity fluctuation over the expansion. This quantity is important because it can be measured in experiments if the collective expansion is precisely identified and subtracted. The cluster local temperature profiles are similar to the local temperature ones. In this way we see that different degrees of freedom are quite thermalized and give similar temperatures. Let us recall once more that in nuclear fragmentation experiments some results show a caloric curve featuring a “gas branch” while others do not; this discrepancy might be explained, as proposed in [1], by considering that different degrees of freedom freeze out at different

temperatures. For our classical system the internal degrees of freedom of the clusters and their c.m. velocity fluctuations around the mean radial velocity yield very similar values of temperatures. The origin of the discrepancies in the experimental nuclear caloric curve might be another; like not taking in account the collective expansion properly in the temperature definition.

The results found for the different temperatures are consistent with our local equilibrium conjecture. If the particle velocity distribution followed:

$$f(\mathbf{v}; \mathbf{r}) = \rho(\mathbf{r}) \left(\frac{m\beta(\mathbf{r})}{2\pi} \right)^{3/2} e^{\beta(\mathbf{r}) \frac{m}{2}(\mathbf{v} - \mathbf{v}_{rad}(\mathbf{r}))^2} \quad (15)$$

all the temperatures defined in this work should yield the same value which is precisely what we found. This is very important fact, because it means that we can know the break-up temperature by measuring the internal temperature of the asymptotic clusters or the cluster local temperature, if the collective motion is properly taken care of, at least for systems similar to the one considered in this study.

Taking the above mentioned into account, we have calculated the extended caloric curve that describes the thermal behavior of our L-J drop from the solid-like regime all the way up to the fragmentation regime. The resulting picture shows the standard behavior up to the liquid-like state. When the energy is further increased leading to evaporation and fragmentation the break-up temperature displays a plateau followed by a monotonous, slow, decrease as the system fragments into smaller and smaller clusters, similar behavior was found in [7,6]. In macroscopic systems a plateau in the caloric curve denotes a phase transition, for example in the solid-liquid phase transition an input of energy will not result in an increase of temperature but in melting. A similar process happens in the solid-like to liquid-like phase transition in small drops [22]. In the case of fragmentation, if the energy of the initial condition is increased the collective expansion will grow, the system will break into smaller fragments but the break-up temperature will not increase.

It is worth mentioning at this point that none of the temperature definitions that we studied show any kind of evidence of the “gas branch” from the fragmentation computer

experiments, which appears as a steady increase of the temperature in the caloric curve, found for high energies in [3]. In our calculations, the cluster internal temperature, the cluster local temperatures and the local temperature slowly decrease as the total energy of the system increases. This can be understood, within our multifragmentation picture taking into account the relation between the temperature of the fragmenting system with the limit temperature of the asymptotic clusters. The remaining energy is converted into collective kinetic energy. The presence of this collective motion is responsible for the break-down of the standard picture of liquid-gas phase transitions. Within our picture of fragmentation no “gas phase” behavior is to be expected, i.e. the temperature will not increase with energy but decrease as the system expands in a more orderly way.

ACKNOWLEDGMENTS

This work was done under partial financial support from the University of Buenos Aires via grant EX-070.

REFERENCES

- [1] J. Pochodzalla, *Prog. Part. Nucl. Phys.* **39**, 443 (1997).
- [2] R. Behrish and K. Wittmaack (eds.), *Sputtering by particle bombardment III* (Springer Verlag Berlin Heidelberg 1991).
- [3] J. Pochodzalla et al. *Phys. Rev. Lett.* **75**, 1040, (1995).
- [4] S. Albergo, S. Costa, E. Costanzo and A. Rubbino, *Nuovo Cimento A* **89**, 1 (1985).
- [5] J. P. Bondorf, O. Friedrichsen, D. Idier and I. N. Mishus in “Critical Phenomena and Collective Observables”, S. Costa, S. Albergo, A. Insolla and C. Tuvè (eds.), World Scientific, Singapore, 1996.
- [6] J. A. Hauger et al., *Phys. Rev. Lett.* **77**, 235 (1996).
- [7] Serfling et. al. (submitted to *Phys. Rev. Lett.*).
- [8] A. Strachan and C. O. Dorso, *Phys. Rev. C* **58**, R632 (1998).
- [9] A. Vicentini, G. Jacucci and V. R. Pandharipande, *Phys. Rev. C* **31**, 1783 (1985).
- [10] R. J. Lenk and V. R. Pandharipande, *Phys. Rev. C* **34**, 177 (1986).
- [11] T. J. Schlagel and V. R. Pandharipande, *Phys. Rev. C* **36**, 162 (1987).
- [12] A. Starchan and C. O. Dorso, *Phys. Rev. C* **55**, 775 (1997).
- [13] Daan Frenkel and Berend Smit, *Understanding Molecular Simulation, from algorithms to applications*, (Academic Press, San Diego, 1996).
- [14] Jean-Pierre Hansen and Loup Verlet, *Phys. Rev.* **184**, 151 (1969).
- [15] D. Stauffer, *Introduction to Percolation Theory*, (Taylor & Francis, London Philadelphia, 1985).
- [16] M. E. Fisher, *Physics (N.Y.)* **3**, 255 (1967); *Rep. Prog. Phys.* **30**, 615 (1967); *Proceedings*

of the International School o Physics, Enrico Fermi Course LI, Critical Phenomena, edited by M.S.Green (Academic Press, New York, 1971).

- [17] M. L. Gilkes et al., Phys. Rev. Lett. **73**, 1590 (1994); J. B. Elliot et al., Phys. Rev. C **49**, 3185 (1994); Phys. Lett. B **381**, 35 (1996).
- [18] A. Strachan and C. O. Dorso, Phys. Rev. C **56**, 995 (1997).
- [19] C. O. Dorso and J. Randrup Phys. Lett B **301**, 328 (1993); C. O. Dorso and J. Aichelin, Phys. Lett. B **345**, 197 (1995); C. O. Dorso and P. Balonga Phys. Rev. C **50**, 991 (1994).
- [20] C. O. Dorso and A. Strachan, Phys. Rev. B **54**, 236 (1996).
- [21] M. Schmidt, R. Kusche, W. Kronmueller, B. von Issendorff, H. Haberland, Phys. Rev. Lett. **79**, 99 (1997).
- [22] Pierre Labastie and Robert L. Whetten, Phys. Rev. Lett. **65**, 1567 (1990). Ralph E. Kunz and R. Stephen Berry, Phys Rev. E **49**, 1895 (1994).
- [23] Kerson Huang, *Statistical Mechanics* (John Wiley & Sons, New York, 1987).

FIGURES

FIG. 1. Asymptotic mass spectra for different initial conditions. (a) $E = 2.2\epsilon$, (b) $E = 1.8\epsilon$, (c) $E = 0.9\epsilon$, (d) $E = 0.5\epsilon$, (e) $E = -0.5\epsilon$, (f) $E = -2\epsilon$. In the cases (a), (b), (c) (d) and (e) the initial density is $\rho = 0.85\sigma^{-3}$ and in (f) it was $\rho = 1\sigma^{-3}$.

FIG. 2. (a) Intermediate mass fragments multiplicities as a function of time for different energies. (b) Mean maximum cluster mass vs. time. Dashed lines join points obtained with the ECRA method while full lines join MST points. Circles denote $E = 1.8\epsilon$, squares denote $E = 0.9\epsilon$, diamonds denote $E = 0.5\epsilon$ and triangles denote $E = -0.5\epsilon$.

FIG. 3. Microscopic persistence coefficient as a function of time for different cases. Full lines denote ECRA results and dashed lines denote MST results. The horizontal lines indicate the evaporation reference, see text. (a) $E = 1.8\epsilon$, (b) $E = 0.9\epsilon$, (c) $E = 0.5\epsilon$ and (d) $E = -0.5\epsilon$.

FIG. 4. Internal temperature of the clusters as a function of their mass number, for asymptotic times (a) and at break-up time (b). Full circles denote $E = 1.8\epsilon$, squares denote $E = 0.9\epsilon$, diamonds denote $E = 0.5\epsilon$ and triangles denote $E = -0.5\epsilon$.

FIG. 5. Total (full lines), collective (dashed-dotted lines) and internal (dashed lines) kinetic energy, and potential energy (dotted lines) as a function of time for different cases. (a) $E = 1.8\epsilon$, (b) $E = 0.9\epsilon$, (c) $E = 0.5\epsilon$ and (d) $E = -0.5\epsilon$.

FIG. 6. Radial velocity profiles at break-up time. Circles denote $E = 1.8\epsilon$, squares denote $E = 0.9\epsilon$, diamonds denote $E = 0.5\epsilon$ and triangles denote $E = -0.5\epsilon$.

FIG. 7. (a) Initial (empty symbols) and break-up (full symbols) local temperature profiles. (b) Break-up (full symbols) and asymptotic (empty symbols) local temperature profiles. Full lines denote $E = 1.8\epsilon$, dotted lines denote $E = 0.9\epsilon$, dashed lines denote $E = 0.5\epsilon$ and dashed-dotted lines denote $E = -0.5\epsilon$.

FIG. 8. Average local temperature of the three innermost regions as a function of time. Dashed-dotted lines denote $E = 1.8\epsilon$, dotted lines denote $E = 0.9\epsilon$, dashed lines denote $E = 0.5\epsilon$ and full lines denote $E = -0.5\epsilon$.

FIG. 9. Energy partition. Total (full lines), collective (dashed-dotted lines) and internal (dashed lines) kinetic energy, potential energy (dotted lines) and average local temperature of the three innermost regions (full thick lines) as a function of the total energy of the system. (a) At asymptotic times and (b) at break-up time.

FIG. 10. Cluster local temperature profiles. Cluster local temperature as a function of distance from the c.m. of the system. Full circles denote $E = 1.8\epsilon$, squares denote $E = 0.9\epsilon$, diamonds denote $E = 0.5\epsilon$ and triangles denote $E = -0.5\epsilon$.

FIG. 11. Extended caloric curve $T(E)$. Regions I, II and III come from the equilibrium simulations. Region IV denotes fragmentation and the average local temperature of the three innermost regions at break-up is plotted.

FIG. 1. A. Strachan & C.O. Dorso. PRC.

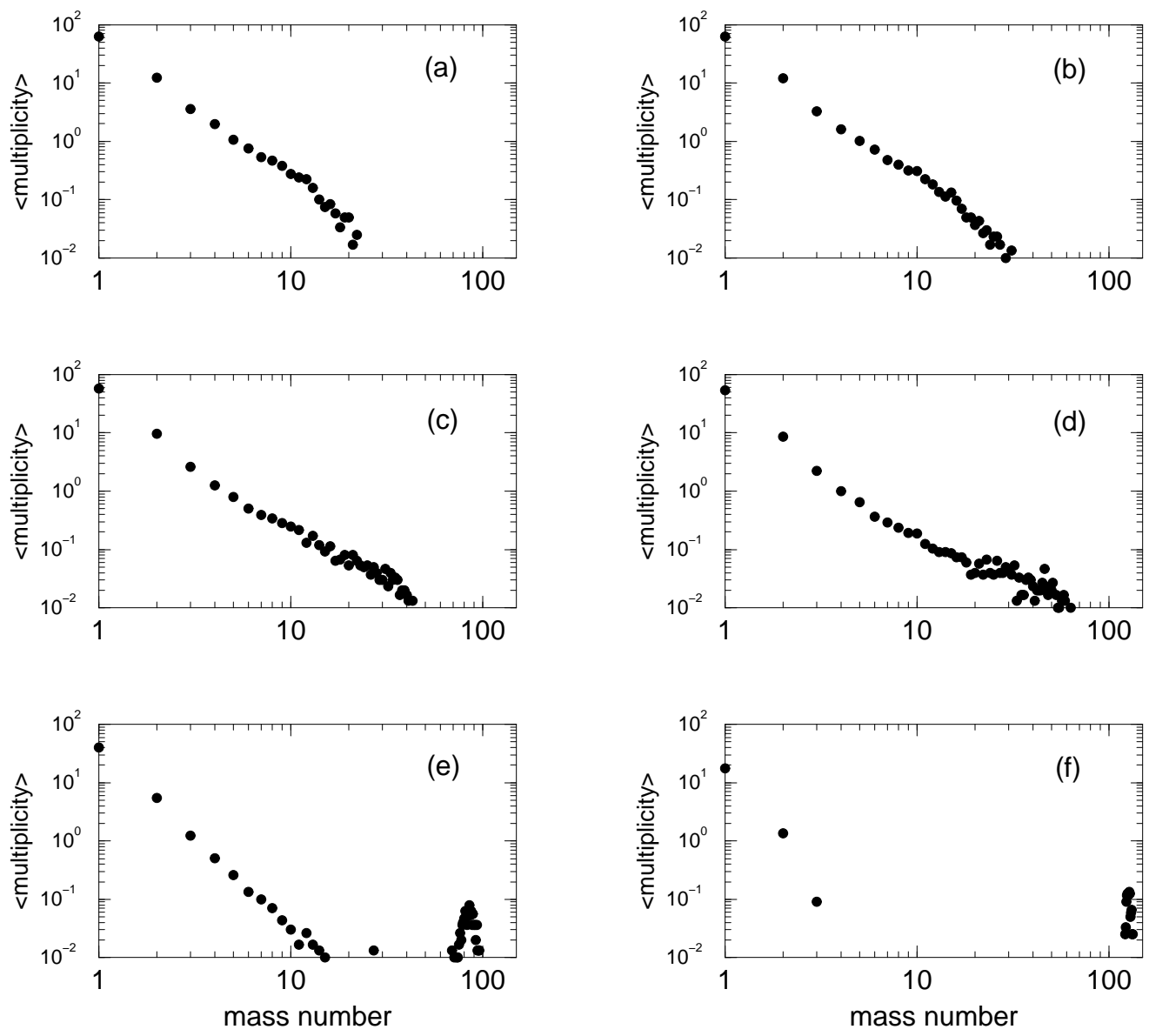


Fig. 2. A. Strachan & C.O.Dorso. PRC.

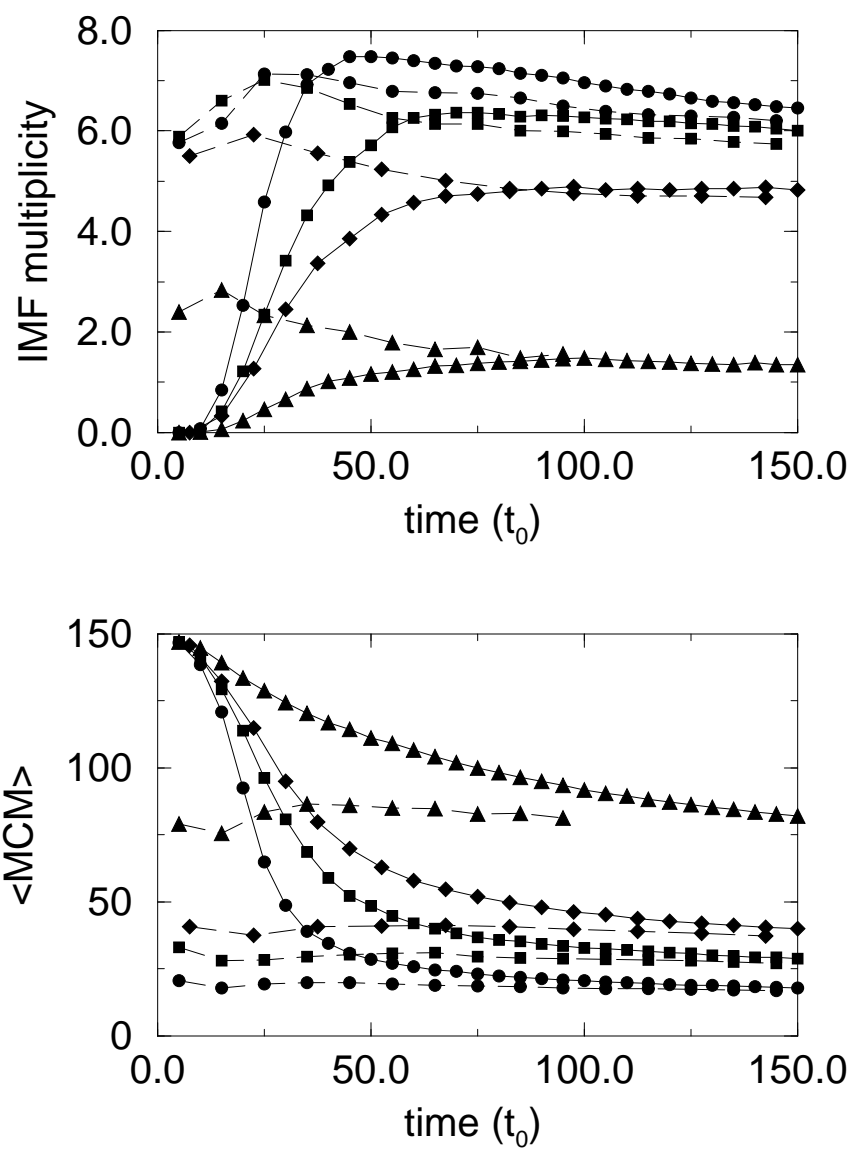


Fig. 2. A.Strachan & C.O.Dorso. PRC.

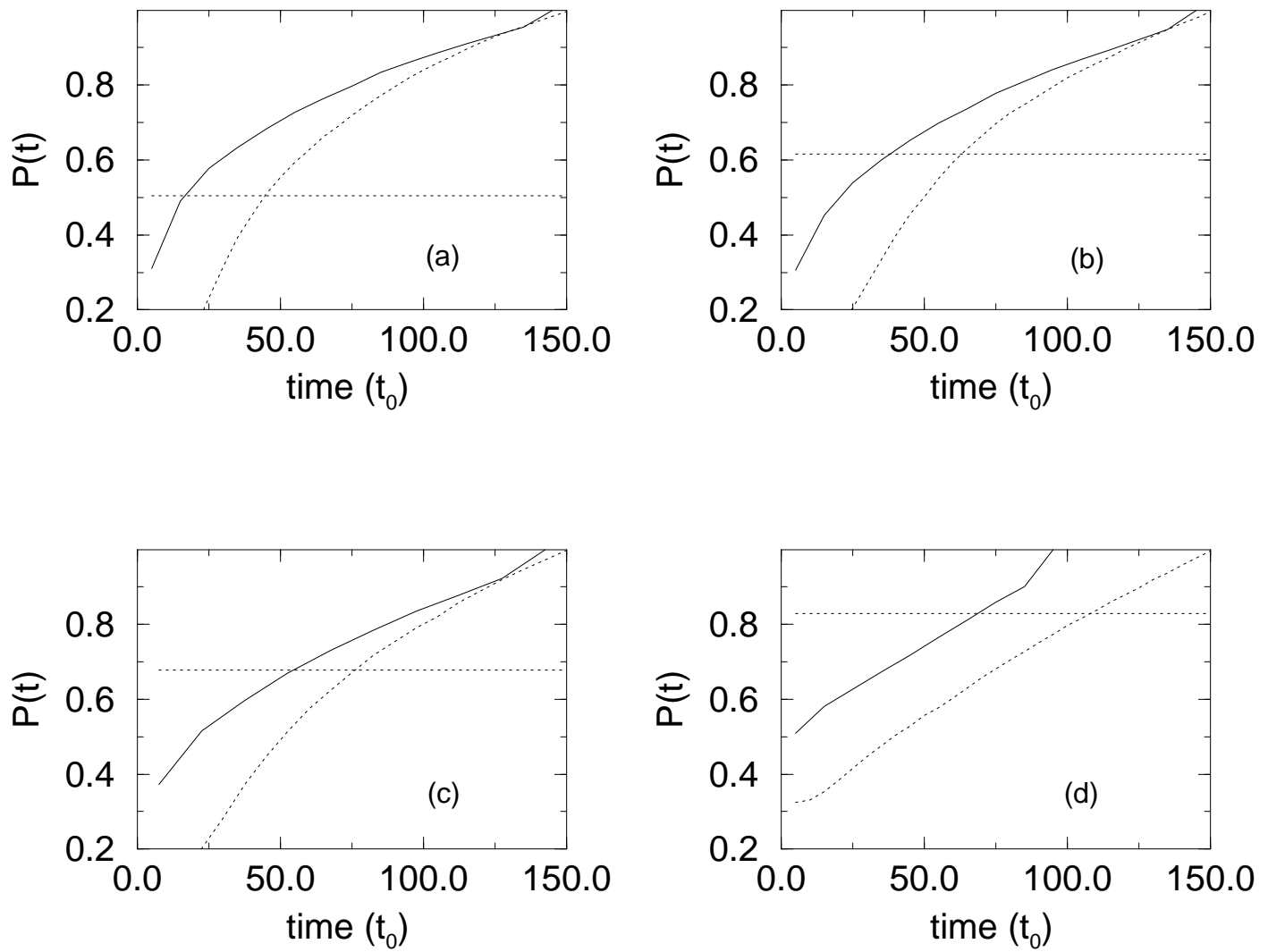


Fig. 4. A.Strachan & C.O.Dorso. PRC

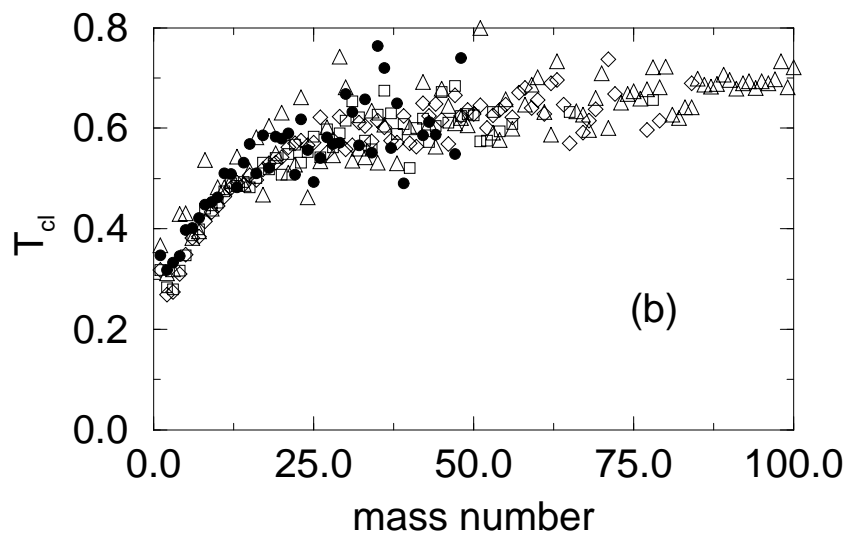
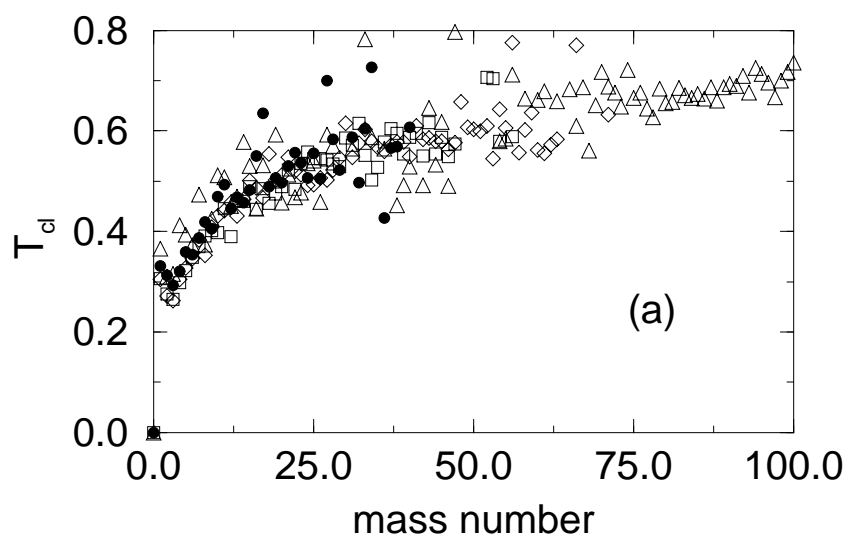


Fig. 6. A.Strachan & C.O.Dorso. PRC.

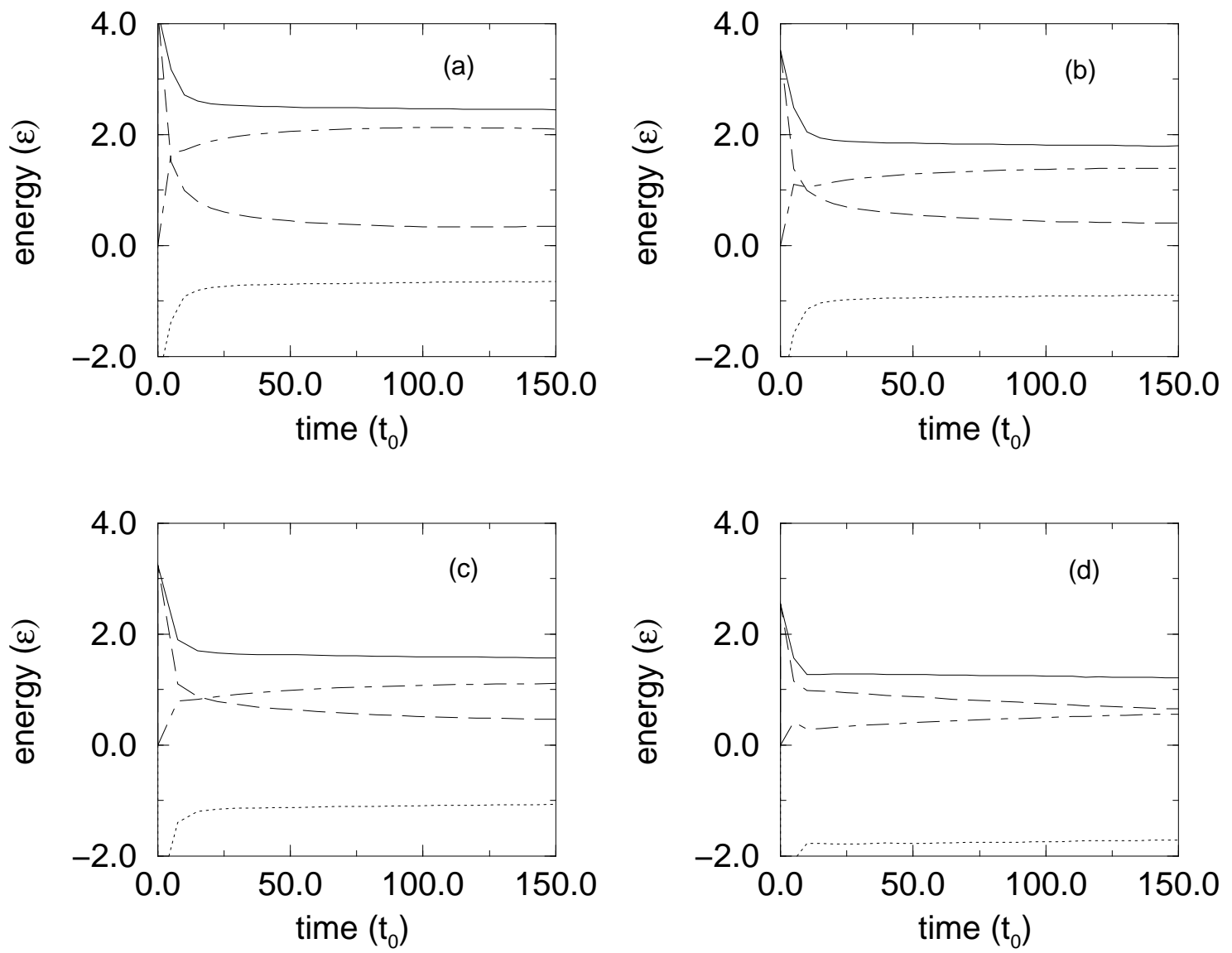


Fig. 6. A.Strachan & C.O.Dorso. PRC.

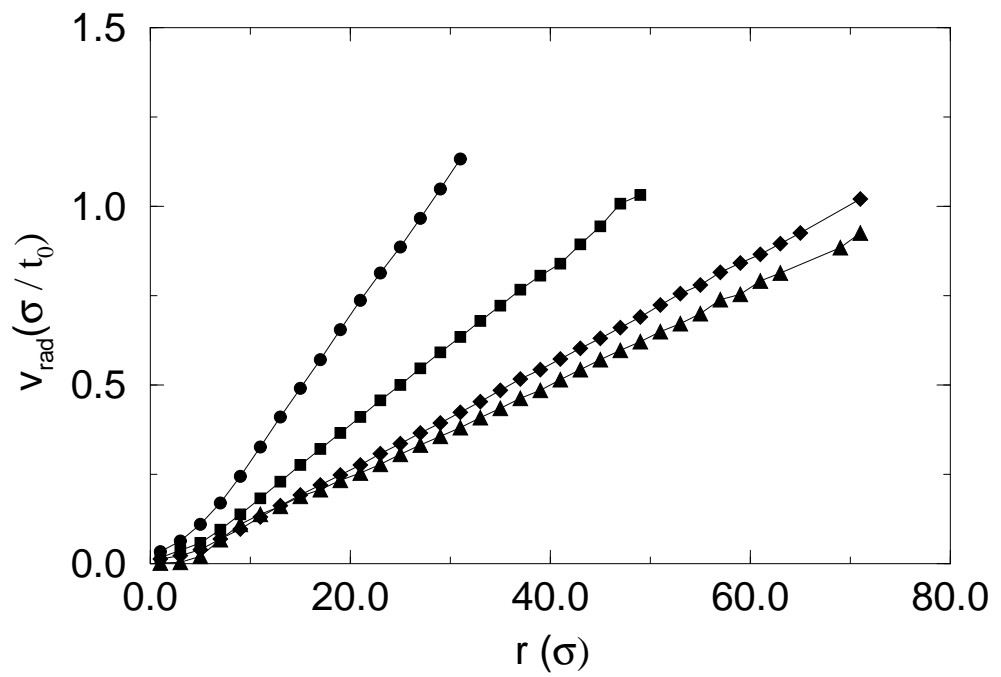


Fig. 7(a). A.Strachan & C.O.Dorso. PRC

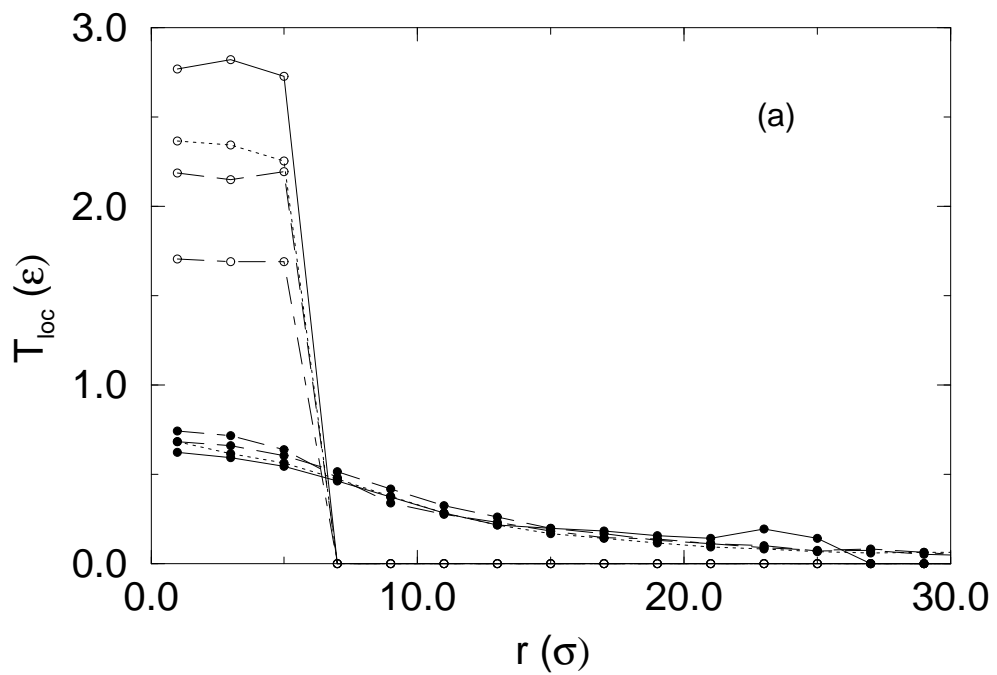


Fig. 7(b). A.Strachan & C.O.Dorso. PRC

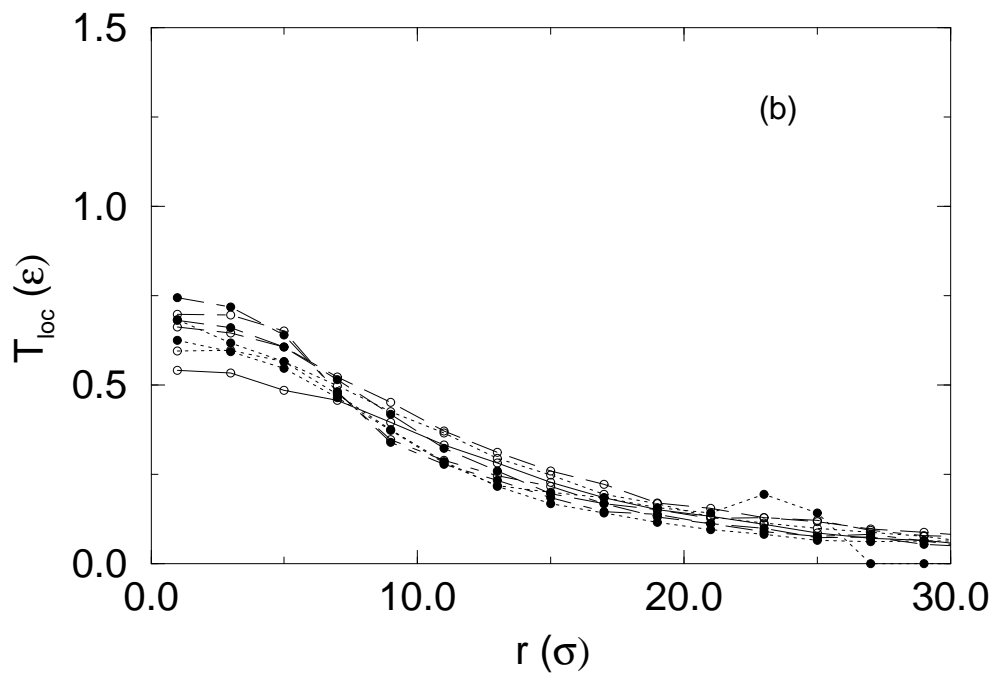


Fig. 8. A. Strachan & C.O. Dorso. PRC.

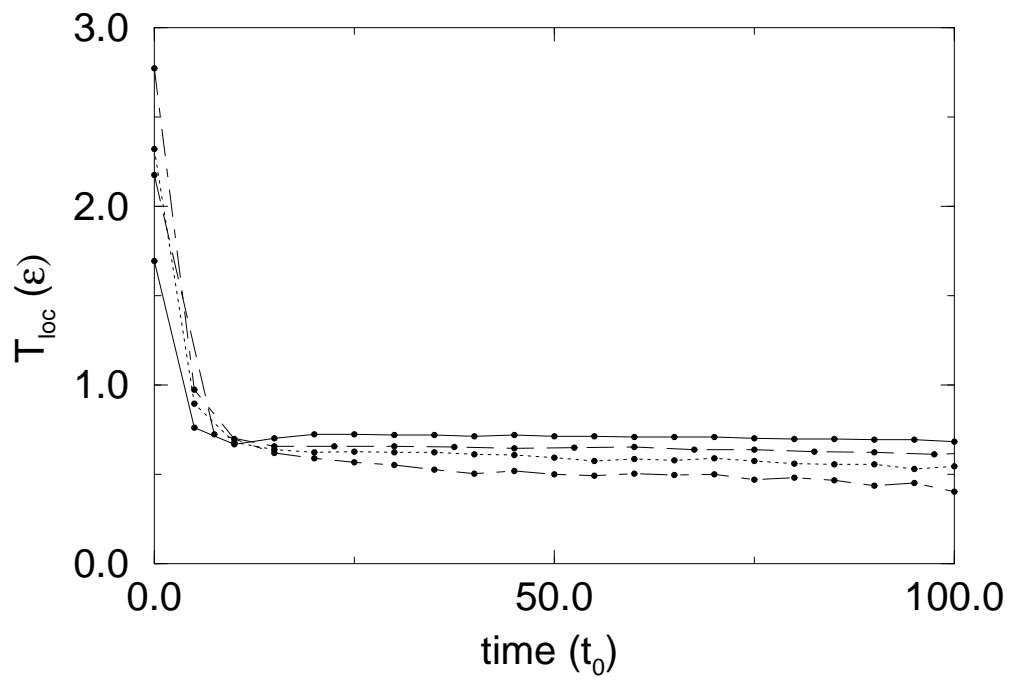


FIG. 9. A.Strachan & C.O. Dorso. PRC.

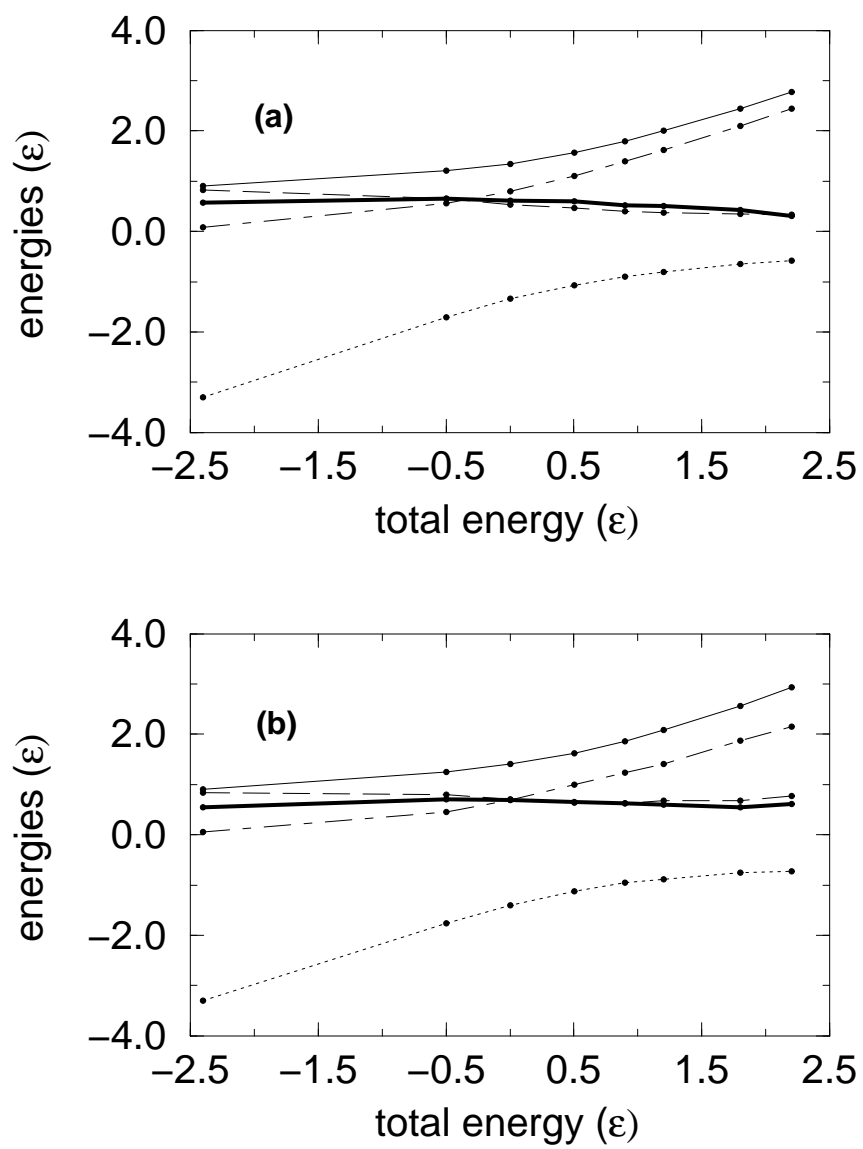


FIG. 10. A.Stracha & C.O.Dorso. PRC.

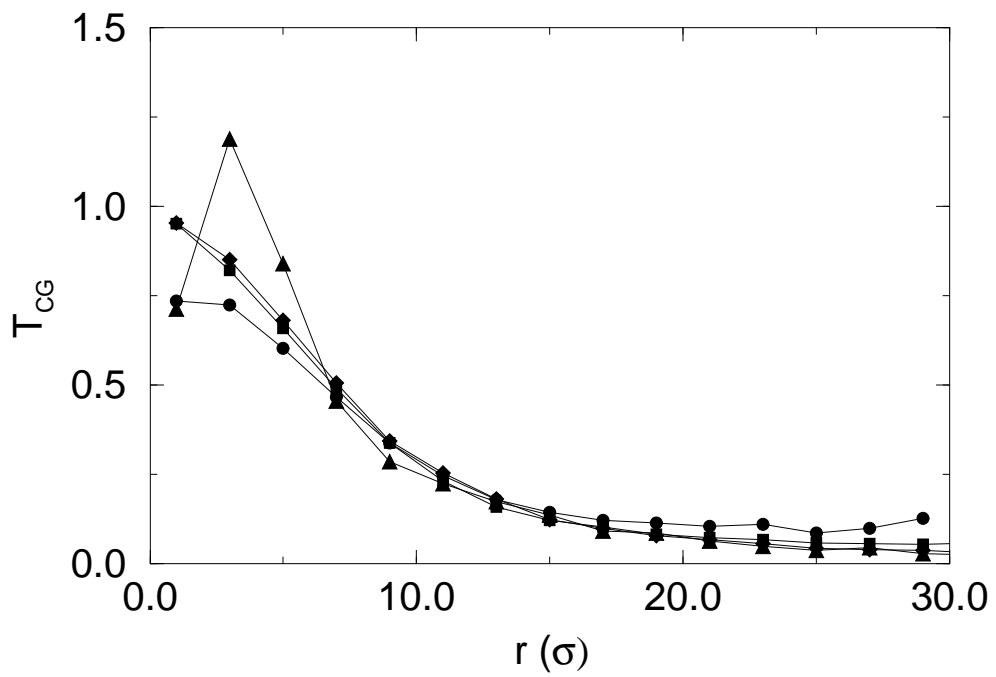


FIG. 11. A. Strachan & C.O. Dorso. PRC.

